Electronic Supplementary Material (ESI) for Physical Chemistry Chemical Physics.

Supplementary Information

Radical Revelations: The Pnictogen Effect in linear Acetylenes

1 Computational methodology benchmark

In order to select the optimal methodology to be employed in the characterization of the here studied systems, the *linear* isomer of DPA was employed as test bed model, as shown in Fig. S1.

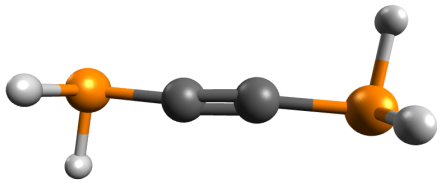

Figure 1: Energetically optimized geometry of the linear isomer of DPA used for bench-marking purposes. Calculations performed at the CCSD/cc-pvTZ in the gas phase.

The geometry was optimized in the gas phase at different levels of theory and the resultant structures were characterized as minima of the PES through the analysis of the characteristic eigenvalues of the Hessian matrix.

Table 1: Comparison of the lowest-Lying vibration mode along with several geometrical features (angles and distances) of the DPA *linear* isomer used as test-bed model computed at different levels of theory in the gas phase.

Methodology	Basis	Freq (cm^{-1})	X-C-C Angle (°)	d(C-C) (Å)	d(C-P) (Å)	d(P-H) (Å)
CCSD	cc-pvTZ	90.54	173.8	1.215	1.781	1.415
B3LYP	def2TZVP	114.36	172.6	1.214	1.762	1.419
B3LYP-GD3	def2TZVP	114.36	172.7	1.214	1.763	1.419
B2PLYP	def2TZVP	107.55	172.8	1.220	1.764	1.414
M062X	def2TZVP	113.84	173.7	1.209	1.768	1.411
PBEPBE	def2TZVP	113.05	171.7	1.227	1.759	1.432
PBEPBE-GD3	def2TZVP	113.03	171.7	1.227	1.759	1.432

As collected in the previous Table, all of the employed levels of theory afforded reasonably equivalent results, providing values of the geometrical features which are quite close to the CCSD/cc-pvTZ data, taken as reference. Based on the obtained results and accounting for the extensive testing and validation which has been carried out on hybrid functionals, the B3LYP functional including Grimme's dispersion correction as implemented in Gaussian09,[1] was selected as the methodology of choice. It should be pointed out that this DFT functional offers a good compromise between accuracy and computational cost. Moreover these, and similar, hybrid functionals have been extensively employed in the literature for the study of a wide variety of simple and complex compounds.

To assess the reliability of the here employed theoretical approach (B3LYP+D3/def2TZVP) in investigating the potential energy surface of DXAs, we optimized the geometries of various isomers presented in the main manuscript using alternative DFT functionals. Specifically, calculations were conducted with the M062X and wB97XD functionals, which should offer an enhanced description of electronic exchange. It's noteworthy that M062X was utilized in combination with the Grimme's GD3 dispersion correction, while wB97XD was applied in its original form, incorporating its inherent dispersion effects. The following figure compiles the energies of the here reported DXAs isomers, relative to the linear conformation, computed at these two distinct levels of theory.

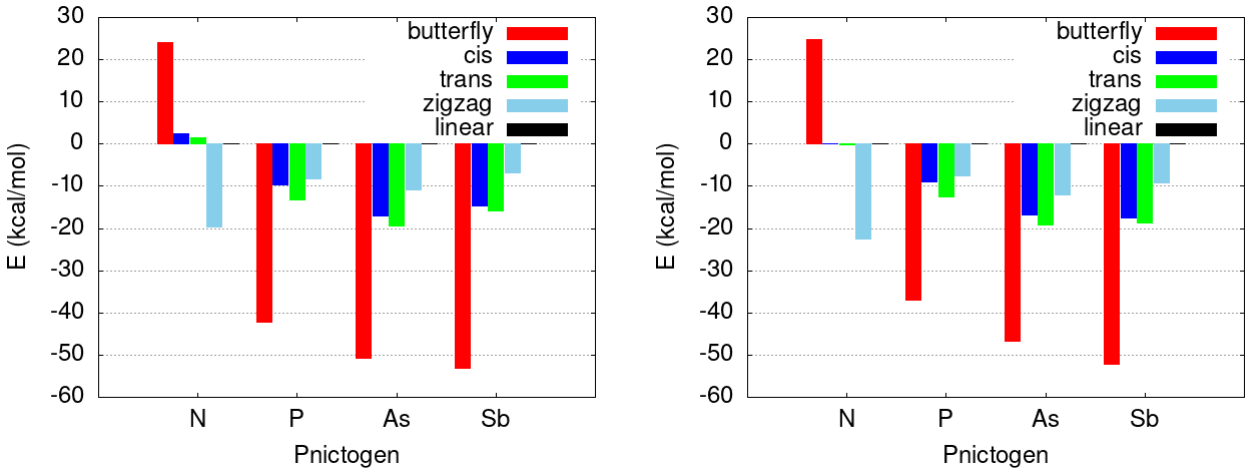

Figure 2: Relative stability, in terms of the electronic energy, of the here considered isomers of DXAs for different pnictogens (X). All the energies are reported, in kcal/ml, relative to the linear (acetylenic) structure. The results for the M062X+GD3/def2-TZVP (left) and wB97XD/def2TZVP (right) are shown.

As can be seen from the latter, all the examined DFT functionals exhibit consistent relative trends, while being in consonance with the selected level of theory used throughout the manuscript. Indeed, the only exception to this general behavior is found for the relative energy difference between the *cis* and *trans* DAA isomers. However, such a discrepancy, characterized by a fairly low offset in the energies well below the 5.0 kcal/mol threshold, is pretty insignificant since none of these system is directly involved in the study presented in our work and hence, it does not alter the conclusions drawn from our results.

2 Tautomerism reactions

2.1 Reaction energy profiles

The current section gathers the reaction energy profiles, reported in terms of the electronic energy, of the gas phase tautomerism reactions of DXAs.

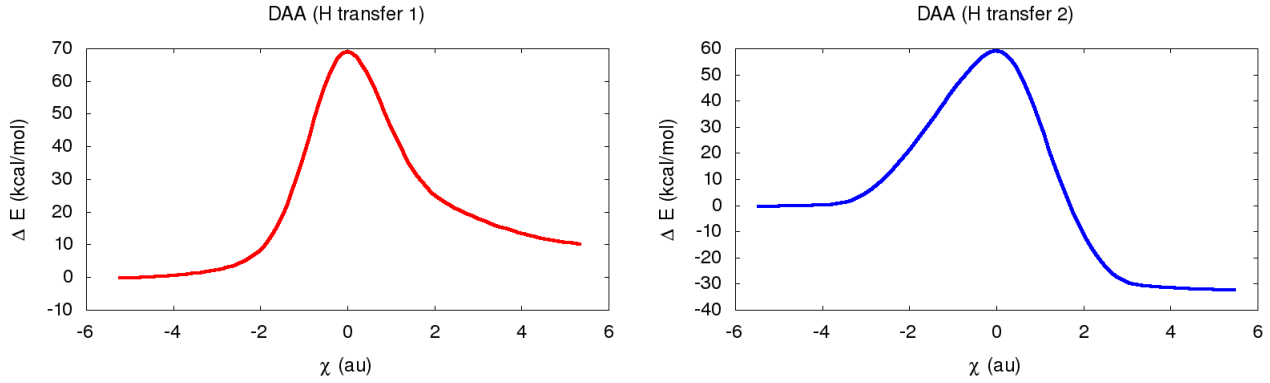

Figure 3: Reaction energy profile, reported in kcal/mol, for the DAA tautomerism reaction under study. All values are reported, as electronic energies, relative to the starting reactant structures.

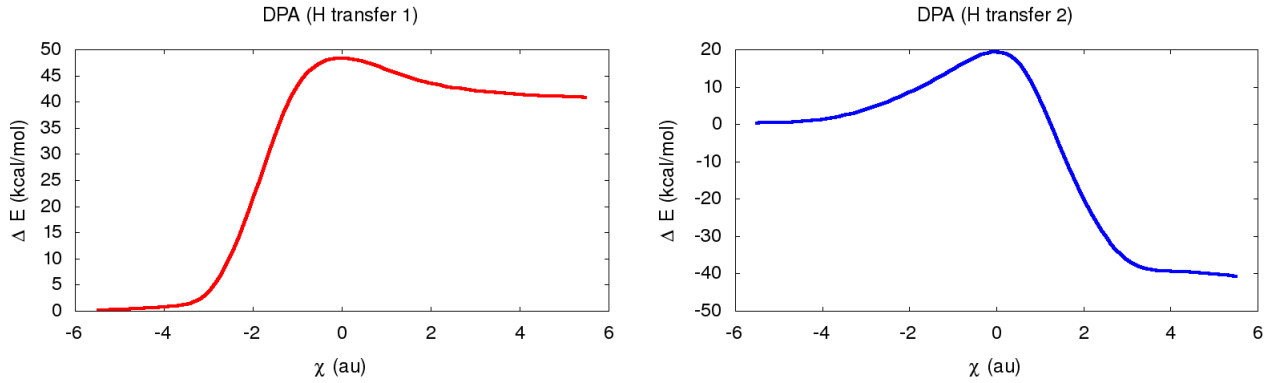

Figure 4: Reaction energy profile, reported in kcal/mol, for the DPA tautomerism reaction under study. All values are reported, as electronic energies, relative to the starting reactant structures.

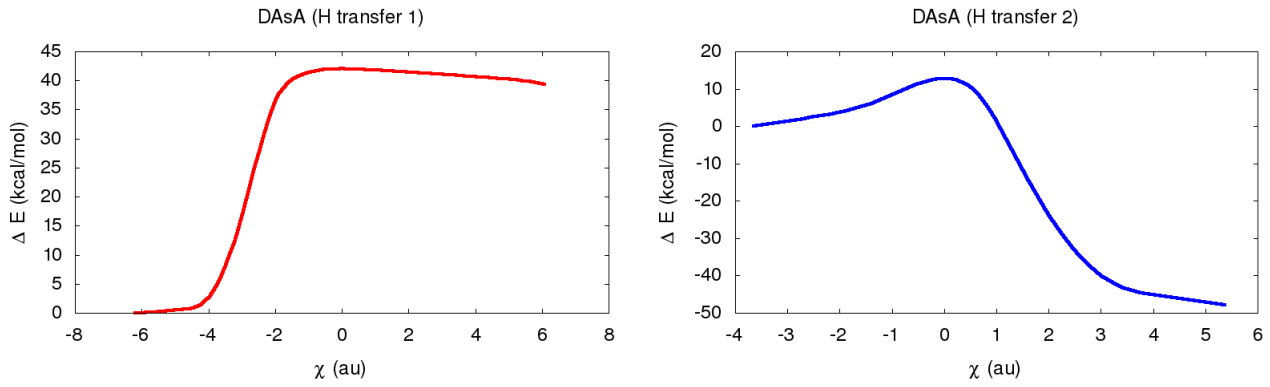

Figure 5: Reaction energy profile, reported in kcal/mol, for the DAsA tautomerism reaction under study. All values are reported, as electronic energies, relative to the starting reactant structures.

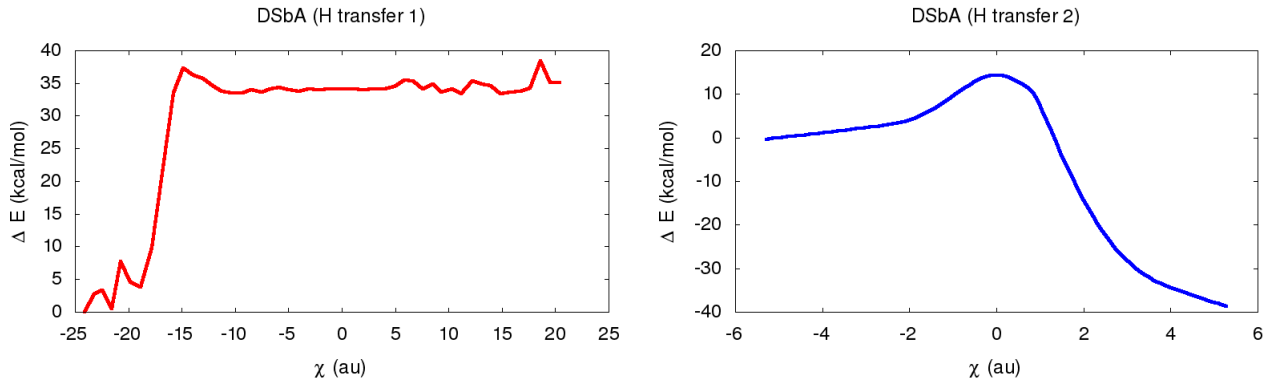

Figure 6: Reaction energy profile, reported in kcal/mol, for the DSbA tautomerism reaction under study. All values are reported, as electronic energies, relative to the starting reactant structures.

The following figures show the reaction energy profiles for the first and second H transfer involved in the DAsA and DSbA tautomerism reactions, accounting for the electrostatically driven ring closure of the reaction intermediates.

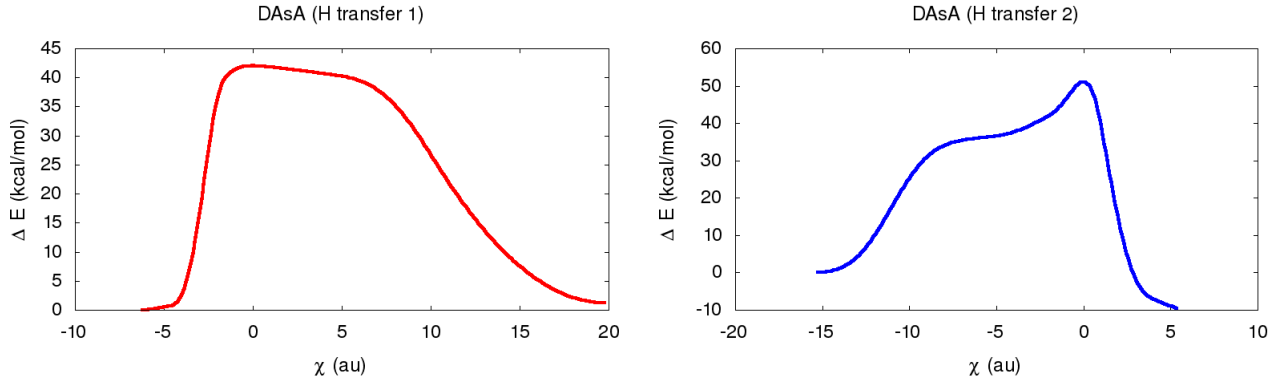

Figure 7: Reaction energy profile, reported in kcal/mol, for the DAsA tautomerism reaction under study accounting for the electrostatically driven ring closure of the intermediate. All values are reported, as electronic energies, relative to the starting reactant structures.

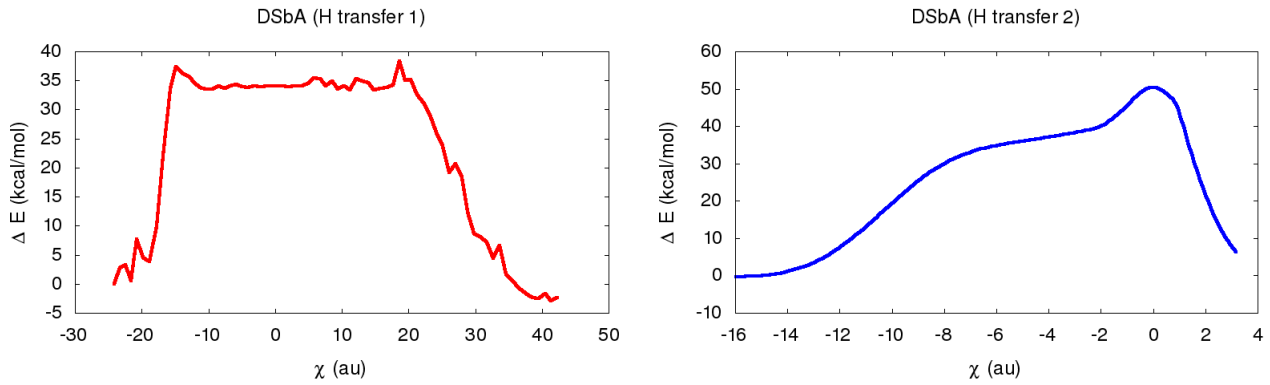

Figure 8: Reaction energy profile, reported in kcal/mol, for the DSbA tautomerism reaction under study accounting for the electrostatically driven ring closure of the intermediate. All values are reported, as electronic energies, relative to the starting reactant structures.

The following figure comprises the energy profiles attributed to the electrostatically driven ring closure of the DAsA and DSbA tautomerism intermediates.

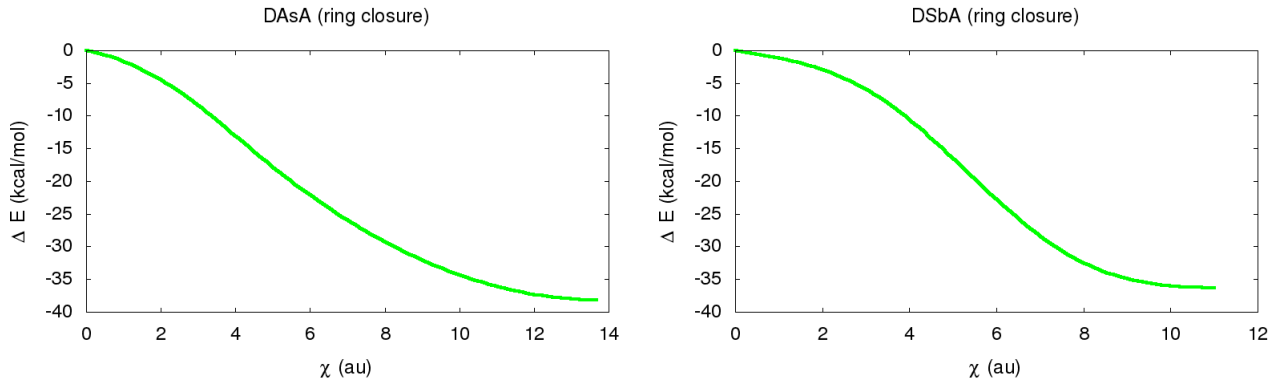

Figure 9: Reaction energy profile, reported in kcal/mol, for the ring closure of the DAsA and DSbA reaction intermediates. All values are reported, as electronic energies, relative to the non-cyclic reaction intermediates.

Similarly, the following table comprises the electronic and Gibbs free energies of the main states involved in the DXAs tautomerism reactions.

Table 2: Electronic (E) and Gibbs free (G) energies, at 298.15 K, of the stationary points involved in the DXA tautomerism. All values are reported in kcal/mol.

Structure	E (kcal/mol)	G (kcal/mol)
DAA *linear*	00.0	00.0
DAA *TS1*	69.1	65.3
DAA *inter*	09.4	09.6
DAA *TS2*	69.3	65.6
DAA *zigzag*	-23.7	-22.8
DPA *linear*	00.0	00.0
DPA *TS1*	48.9	47.6
DPA *inter*	38.0	38.8
DPA *TS2*	58.9	58.4
DPA *zigzag*	-10.1	-05.9
DAsA *linear*	00.0	00.0
DAsA *TS1*	42.5	41.9
DAsA *inter*	38.1	39.6
DAsA *inter-ring*	01.7	03.7
DAsA *TS2*	52.7	53.2
DAsA *zigzag*	-16.5	-11.3
DSbA *linear*	00.0	00.0
DSbA *TS1*	34.7	35.6
DSbA *inter*	33.3	34.8
DSbA *inter-ring*	-02.7	00.3
DSbA *TS2*	48.0	49.5
DSbA *zigzag*	-16.5	-10.1

The following figures comprise a representation of the steady states involved in the DXA tautomerism.

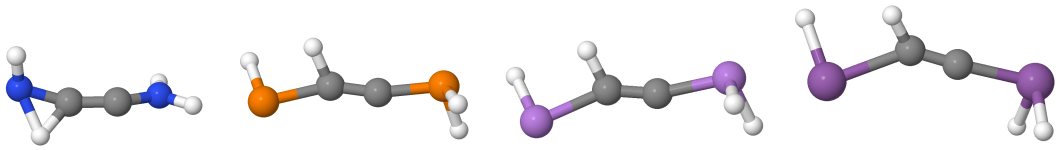

Figure 10: Representation of the transition states for the first H transfer of the DAA, DPA, DAsA and DSbA tautomerism reactions.

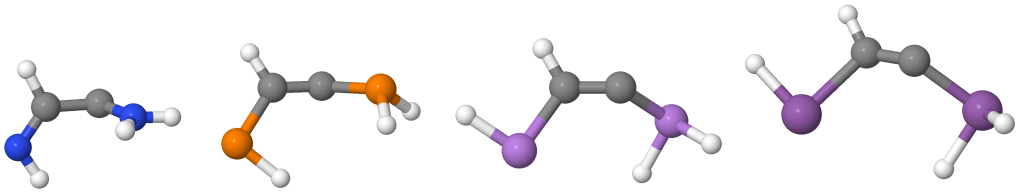

Figure 11: Representation of the intermediate of the DAA, DPA, DAsA and DSbA tautomerism reactions.

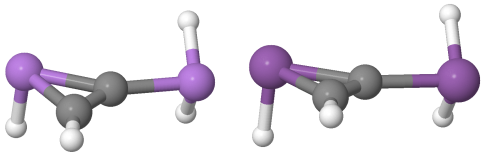

Figure 12: Representation of the cyclic intermediates of the DAsA and DSbA tautomerism reactions.

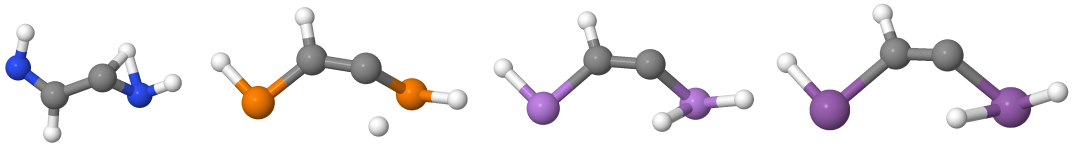

Figure 13: Representation of the transition states for the second H transfer of the DAA, DPA, DAsA and DSbA tautomerism reactions.

2.2 Evolution of QTAIM metrics throughout the tautomerism reaction

The following figures comprise the evolution of the QTAIM metrics of the main atoms and bonds involved in the first H transfer of the DXAs tautomerism reactions.

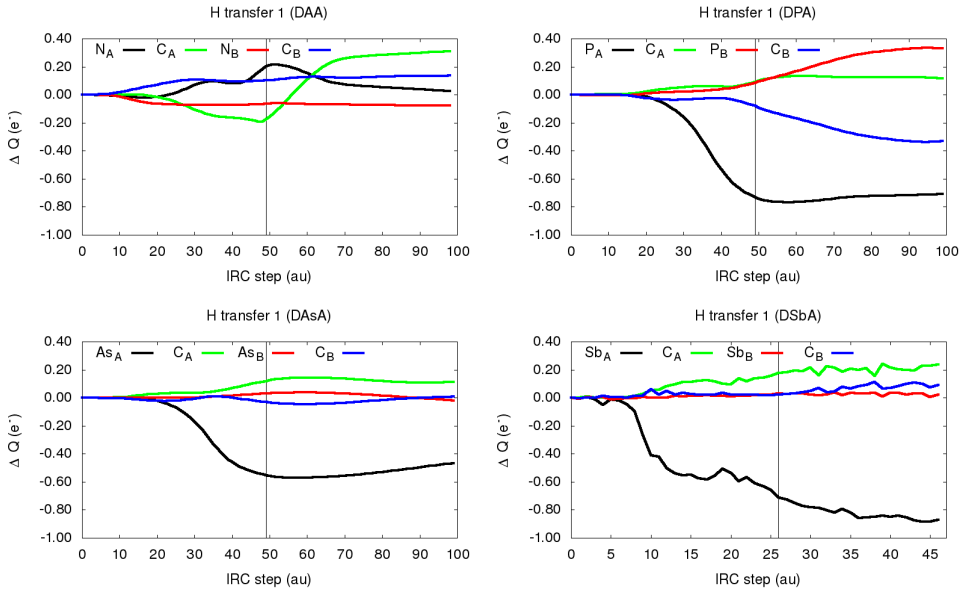

Figure 14: Evolution of the QTAIM atomic charges (Q) for the main atoms participating in the first H transfer of the DAA, DPA, DAsA and DSbA tautomerism reactions. All values are reported, in electrons, relative to the starting reactive complex. The reference values for the X_A, C_A, X_B and C_B atoms are : [-1.10, 0.33, -1.10, 0.33], [1.68, -0.70, 1.68, -0.71], [1.05, -0.49, 1.05, -0.50] and [1.15, -0.51, 1.15, -0.52] for DAA, DPA, DAsA and DSbA, respectively.

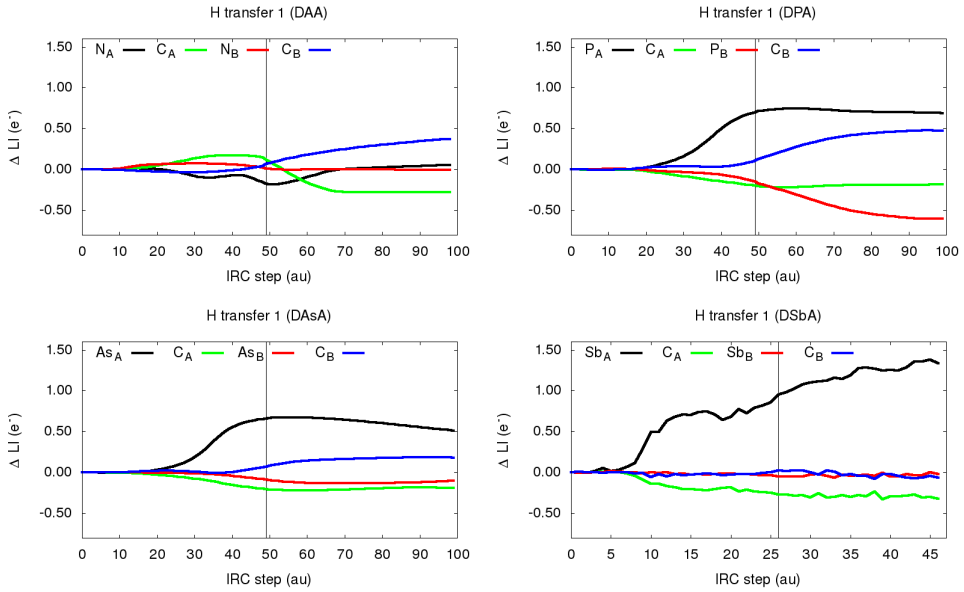

Figure 15: Evolution of the localization index (λ) for the main atoms participating in the first H transfer of the DAA, DPA, DAsA and DSbA tautomerism reactions. All values are reported, in electrons, relative to the starting reactive complex. The reference values for the X_A, C_A, X_B and C_B atoms are: [6.57, 3.71, 6.57, 3.71], [11.98, 4.73, 11.98, 4.73], [30.46, 4.51, 30.46, 4.51] and [20.39, 4.56, 20.40, 4.57] for DAA, DPA, DAsA and DSbA, respectively.

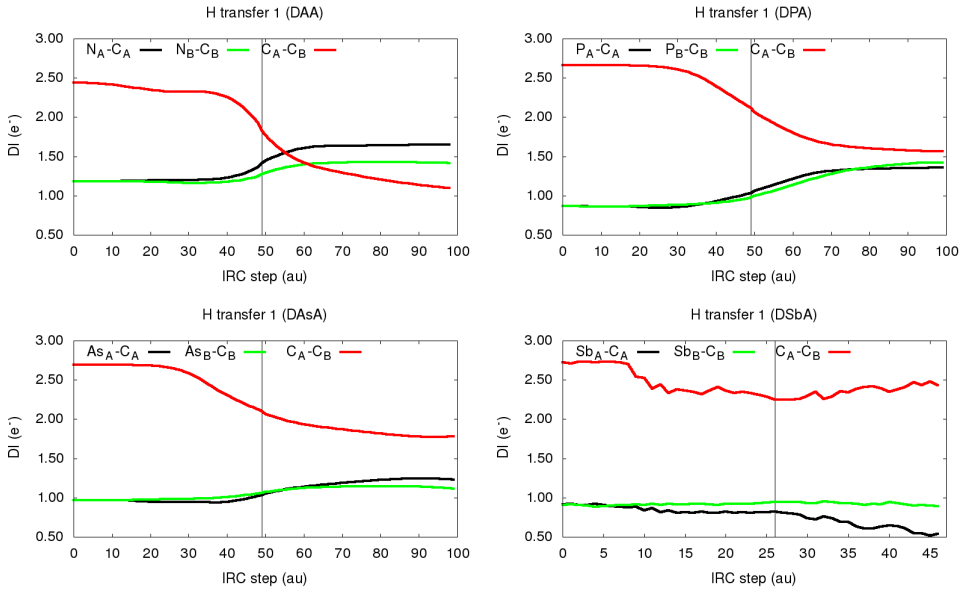

Figure 16: Evolution of the delocalization index (δ) for the main bonds participating in the first H transfer of the DAA, DPA, DAsA and DSbA tautomerism reactions. All values are reported, in electrons, relative to the starting reactive complex.

The following figures comprise the evolution of the QTAIM metrics of the main atoms and bonds involved in the second H transfer of the DXAs tautomerism reactions.

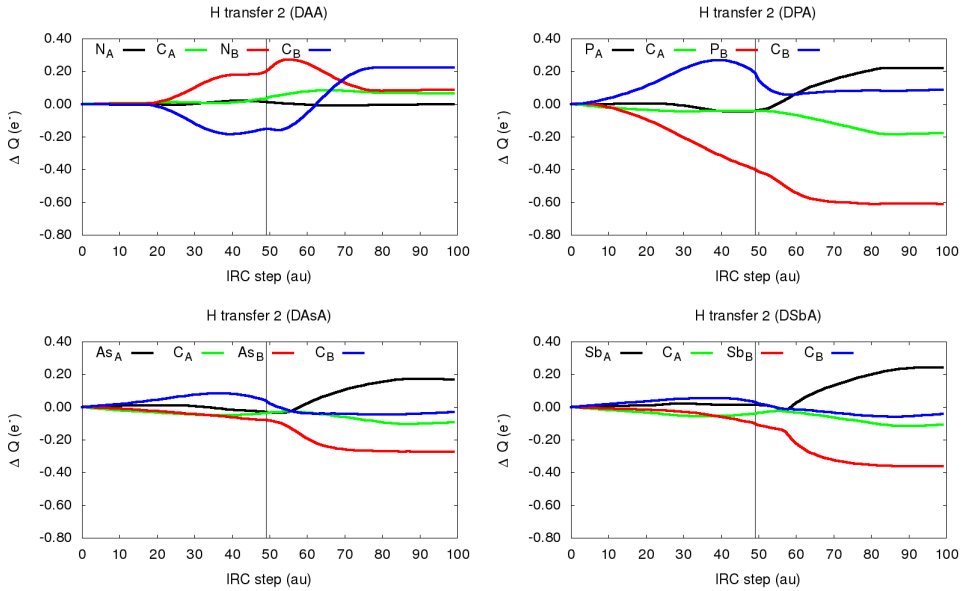

Figure 17: Evolution of the QTAIM atomic charges (Q) for the main atoms participating in the second H transfer of the DAA, DPA, DAsA and DSbA tautomerism reactions. All values are reported, in electrons, relative to the starting reactive complex. The reference values for the X_A, C_A, X_B and C_B atoms are: [-1.08, 0.64, -1.17, 0.47], [1.07, -0.66, 1.90, -0.93], [0.57, -0.41, 1.01, -0.47] and [0.53, -0.38, 1.13, -0.45] for DAA, DPA, DAsA and DSbA, respectively.

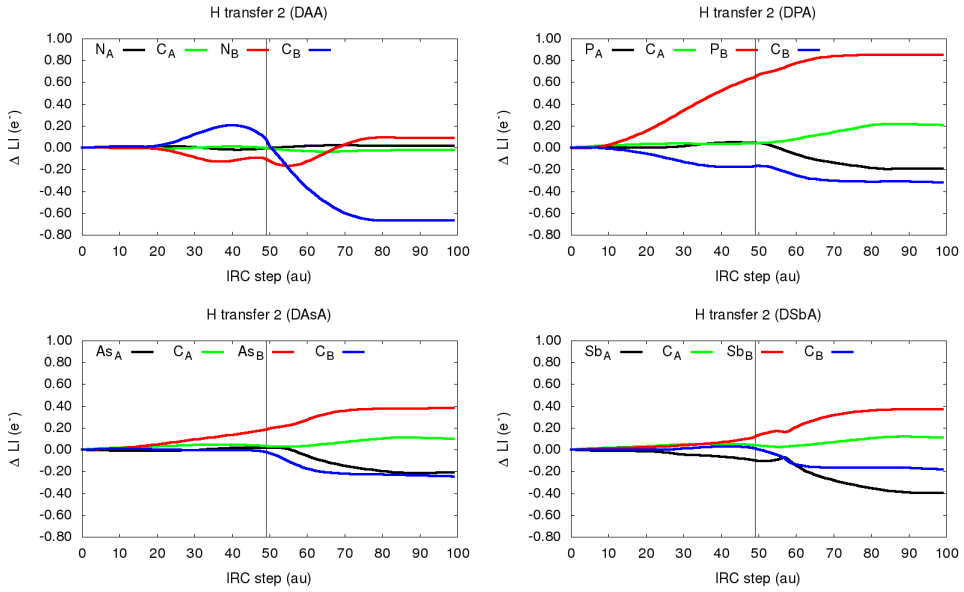

Figure 18: Evolution of the localization index (λ) for the main atoms participating in the second H transfer of the DAA, DPA, DAsA and DSbA tautomerism reactions. All values are reported, in electrons, relative to the starting reactive complex. The reference values for the X_A, C_A, X_B and C_B atoms are: [6.63, 3.44, 6.56, 4.09], [12.56, 4.62, 11.52, 5.15], [30.98, 4.35, 30.39, 4.70] and [21.14, 4.34, 20.39, 4.63] for DAA, DPA, DAsA and DSbA, respectively.

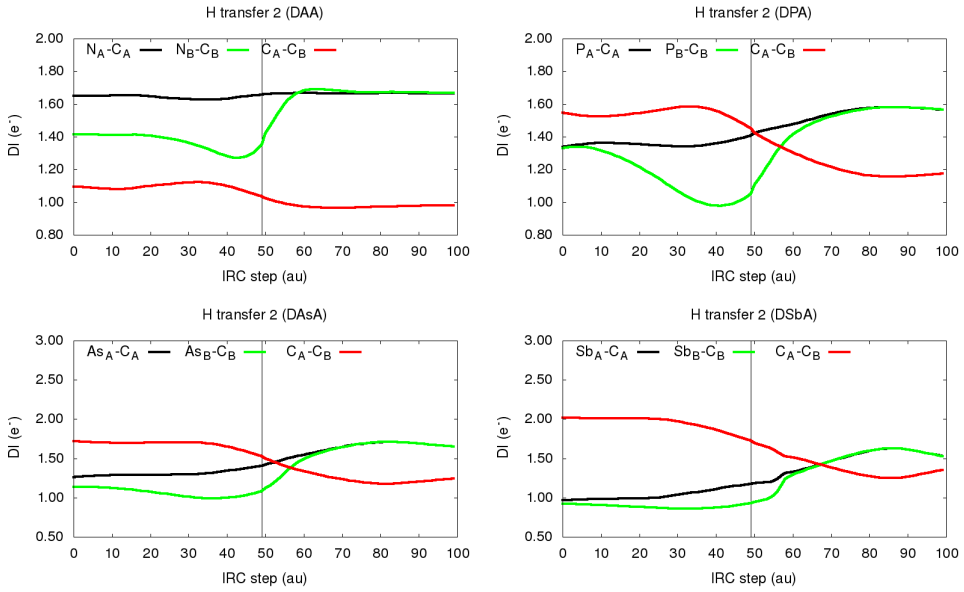

Figure 19: Evolution of the delocalization index (δ) for the main bonds participating in the second H transfer of the DAA, DPA, DAsA and DSbA tautomerism reactions. All values are reported, in electrons, relative to the starting reactive complex.

Similarly, the following figures show the evolution of the delocalization index of the C-H and X-H bonds throughout the DAA and DPA tautomerism reactions.

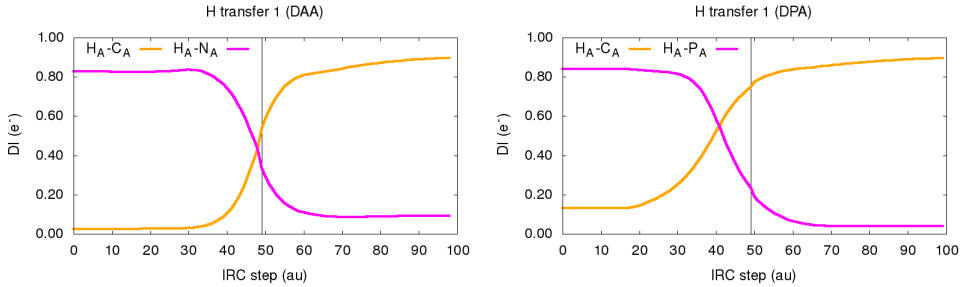

Figure 20: Evolution of the delocalization index (δ) for the C-H and X-H bonds getting formed and broken, respectively, throughout the first H transfer involved in the DAA and DPA tautomerism reactions. All values are reported, in electrons, relative to the starting reactive complex.

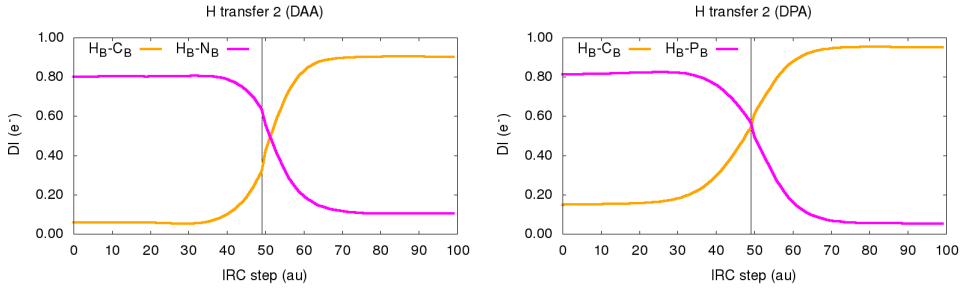

Figure 21: Evolution of the delocalization index (δ) for the C-H and X-H bonds getting formed and broken, respectively, throughout the second H transfer involved in the DAA and DPA tautomerism reactions. All values are reported, in electrons, relative to the starting reactive complex.

Finally, the following figures show the evolution of the QTAIM metrics throughout the DAsA and DSbA intramolecular ring closure reactions.

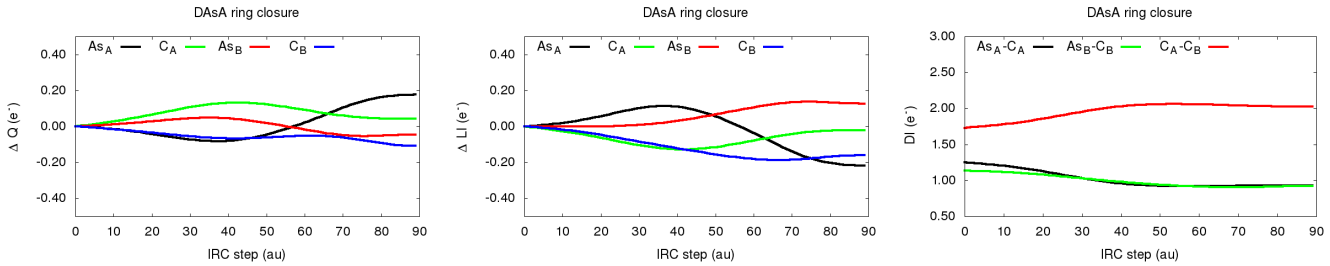

Figure 22: Evolution of the change in atomic charges (left), localization (center) and delocalization (right) indices for the main atoms and bonds involved in the DAsA ring closure phenomenon. All values are reported, in electrons, relative to the starting non-cyclic intermediate.

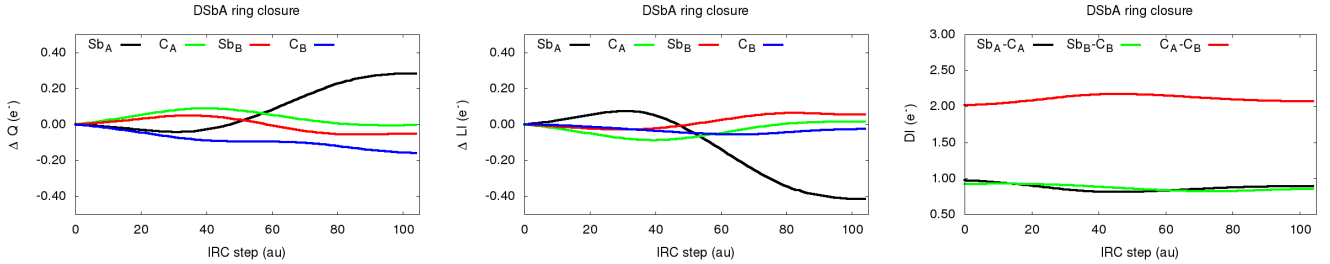

Figure 23: Evolution of the change in atomic charges (left), localization (center) and delocalization (right) indices for the main atoms and bonds involved in the DSbA ring closure phenomenon. All values are reported, in electrons, relative to the starting non-cyclic intermediate.

2.3 Topological analysis of the ELF

Reaction intermediates

The current section comprises the volumes and populations of the ELF basins of the reaction intermediates involved in the DXAs tautomerism.

Table 3: ELF basin volumes (V) and populations (N) for the intermediate involved in the DAA tautomerism. All values are given in electrons or Å^3 for the basin populations and volumes, respectively.

Basin	V	N
C(C_A)	0.8	2.09
C(C_B)	0.8	2.09
C(N_B)	0.4	2.11
C(N_A)	0.5	2.11
V(H-N_B)	63.6	2.04
V(H-N_B)	62.1	2.05
V(H-N_A)	62.8	1.96
V(H-C_A)	86.6	2.12
V(C_B-C_A)	22.9	2.16
V(C_A-N_A)	46.7	2.78
V(C_B-N_B)	72.3	3.54
V(C_B)	129.8	2.11
V(N_A)	119.5	2.83
V(N_B)	–	–

Table 4: ELF basin volumes (V) and populations (N) for the intermediate involved in the DPA tautomerism. All values are given in electrons or Å^3 for the basin populations and volumes, respectively.

Basin	V	N
C(C_A)	0.8	2.09
C(C_B)	0.8	2.09
C(P_B)	4.6	10.06
C(P_A)	4.5	10.05
V(H-P_B)	100.6	1.98
V(H-P_B)	102.7	1.98
V(H-P_A)	99.6	2.01
V(H-C_A)	81.1	2.06
V(C_B-C_A)	32.2	2.41
V(C_A-P_A)	46.8	2.41
V(C_B-P_B)	41.2	2.26
V(C_B)	96.4	1.77
V(P_A)	265.2	3.16
V(P_B)	130.7	1.66

Table 5: ELF basin volumes (V) and populations (N) for the intermediate involved in the DAsA tautomerism. All values are given in electrons or Å^3 for the basin populations and volumes, respectively.

Basin	V	N
C(C_A)	0.8	2.09
C(C_B)	0.8	2.09
C(As_B)	8.5	27.71
C(As_A)	8.4	27.7
V(H-As_B)	108.4	1.98
V(H-As_B)	112.2	1.99
V(H-As_A)	116.4	2.01
V(H-C_A)	78.5	2.05
V(C_B-C_A)	41.7	2.66
V(C_A-As_A)	48.2	2.19
V(C_B-As_B)	32.5	1.88
V(C_B)	106.3	1.86
V(As_A)	282.1	3.55
V(As_B)	166.6	2.22

Table 6: ELF basin volumes (V) and populations (N) for the intermediate involved in the DSbA tautomerism. All values are given in electrons or Å^3 for the basin populations and volumes, respectively. Since pseudo-potentials were employed in the computation of DSbA systems, the ELF basins attributed to the Sb cores have been omitted.

Basin	V	N
C(C_A)	0.8	2.09
C(C_B)	0.8	2.08
C(Sb_B)	–	–
C(Sb_A)	–	–
V(H-Sb_B)	125.8	1.95
V(H-Sb_B)	132.2	1.96
V(H-Sb_A)	139.7	1.97
V(H-C_A)	78.4	2.07
V(C_B-C_A)	60.0	3.07
V(C_A-Sb_A)	43.2	1.74
V(C_B-Sb_B)	35.3	1.71
V(C_B)	98.3	1.67
V(Sb_A)	366.2	3.71
V(Sb_B)	206.0	2.30

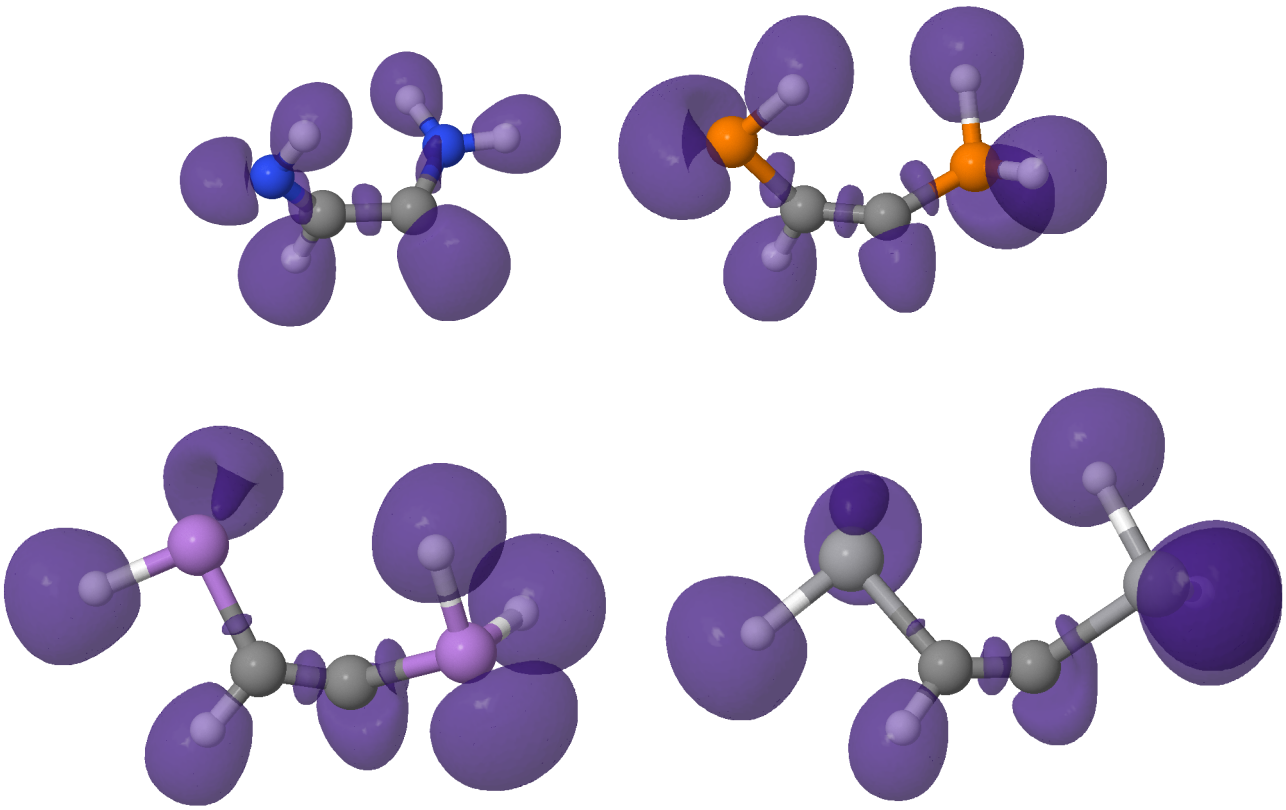

Figure 24: ELF of the DAA, DPA, DAsA and DSbA tautomerism intermediates. An isovalue of 0.86 units was employed for the representation.

Transition states of the first H transfer

The following figures show the ELF isosurfaces, along with the volumes and populations of the corresponding basins, of the transition states involved in the first H transfer of the DAA and DPA tautomerism reactions.

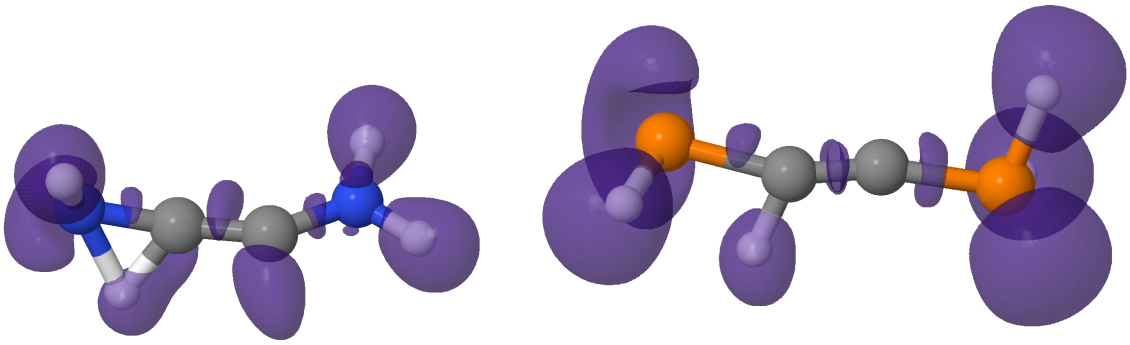

Figure 25: ELF isosurface of the DAA (left) and DPA (right) transition states of the first H transfer involved in the tautomerism reactions. An isovalue of 0.86 units was employed for the representation.

Table 7: ELF basin volumes (V) and populations (N) for the first transition state involved in the DAA (left) and DPA (right) tautomerism. All values are given in electrons or Å^3 for the basin populations and volumes, respectively.

Basin	V	N	V	N
C(C_A)	0.8	2.10	0.8	2.09
C(C_B)	0.8	2.09	0.8	2.09
C(X_B)	0.4	2.11	4.6	10.06
C(X_A)	0.4	2.10	4.6	10.05
V(H-X_B)	62.3	1.94	100.9	1.95
V(H-X_B)	60.9	1.94	101.5	1.96
V(H-X_A)	66.4	1.96	101.1	1.97
V(H-C_A-X_A)	94.1	2.12	59.9	1.76
V(C_B-C_A)	50.6	2.92	49.9 // 58.2	1.73 // 2.16
V(C_A-X_A)	17.2	1.87	33.6	1.97
V(C_B-X_B)	14.7	1.94	78.8	2.99
V(C_B)	91.6	1.65	–	–
V(X_A)	124.6	3.35	264.1	3.29
V(X_B)	30.0 // 36.9	0.87 // 1.02	148.4	1.91

Transition states of the second H transfer

The following figures show the ELF isosurfaces, along with the volumes and populations of the corresponding basins, of the transition states involved in the second H transfer of the DAA and DPA tautomerism reactions.

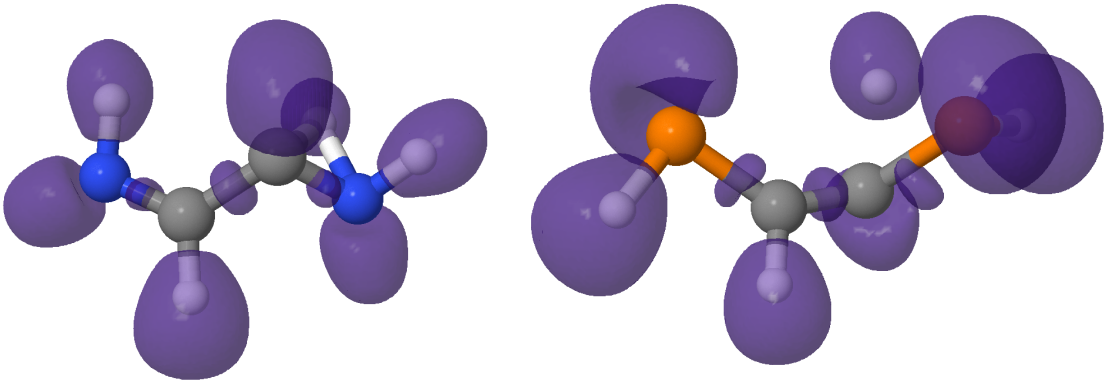

Figure 26: ELF isosurface of the DAA (left) and DPA (right) transition states of the second H transfer involved in the tautomerism reactions. An isovalue of 0.86 units was employed for the representation.

Table 8: ELF basin volumes (V) and populations (N) for the second transition state involved in the DAA (left) and DPA (right) tautomerism. All values are given in electrons or $Å^3$ for the basin populations and volumes, respectively.

Basin	V	N	V	N
$C(C_A)$	0.8	2.1	0.8	2.10
$C(C_B)$	0.8	2.08	0.8	2.08
$C(X_B)$	0.5	2.11	4.6	10.05
$C(X_A)$	0.4	2.1	4.5	10.05
$V(H\text{-}X_B)$	57.7	1.97	101.6	2.01
$V(H\text{-}X_A)$	61.5	1.97	105.2	2.00
$V(H\text{-}C_B\text{-}X_B)$	53.1	1.29	67.1	1.61
$V(C_B\text{-}C_A)$	23.0	2.12	25.1	2.30
$V(C_A\text{-}X_A)$	57.5	2.89	54.8	2.57
$V(C_B\text{-}X_B)$	19.6	1.93	34.8	1.90
$V(C_B)$	120.6	2.06	97.2	1.86
$V(X_A)$	109.3	2.67	263.8	3.18
$V(X_B)$	92.8	2.56	170.0	2.23
$V(H\text{-}C_A)$	85.2	2.14	77.3	2.03

2.4 Analysis of the local spin $< S_A^2 >$

First H transfer

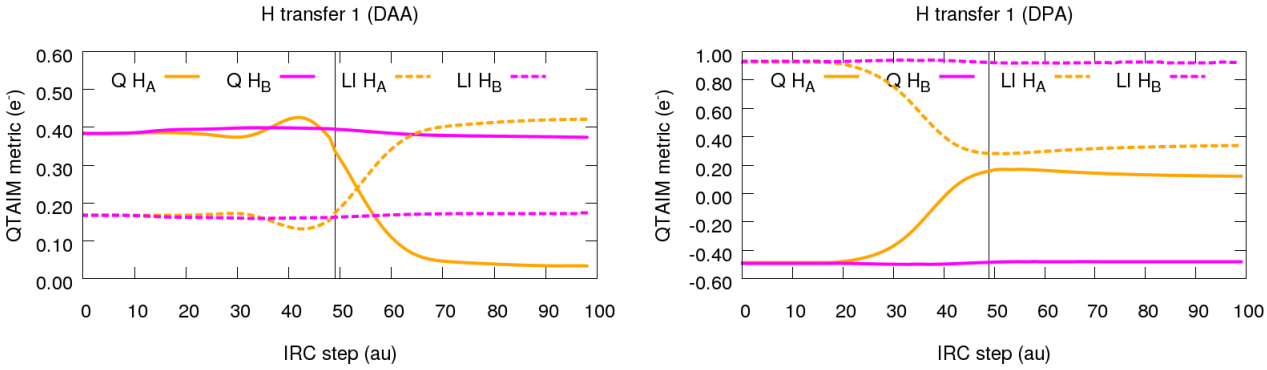

Figure 27: Evolution of the localization index (LI) and atomic charge (Q) of the H_A and H_B atoms throughout the first H transfer involved in the DAA and DPA tautomerism.

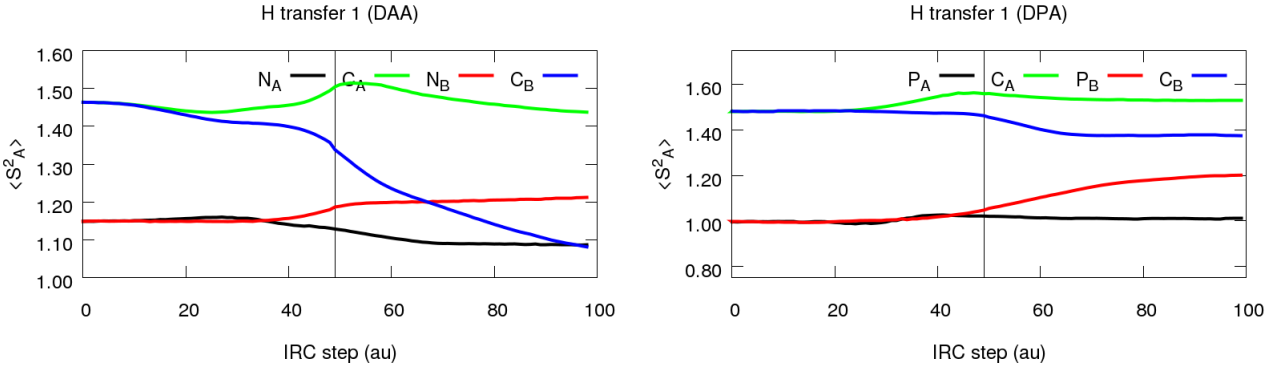

Figure 28: Evolution of the local spin, $< S_A^2 >$, of the main atoms involved in the first H transfer of the DAA and DPA tautomerism.

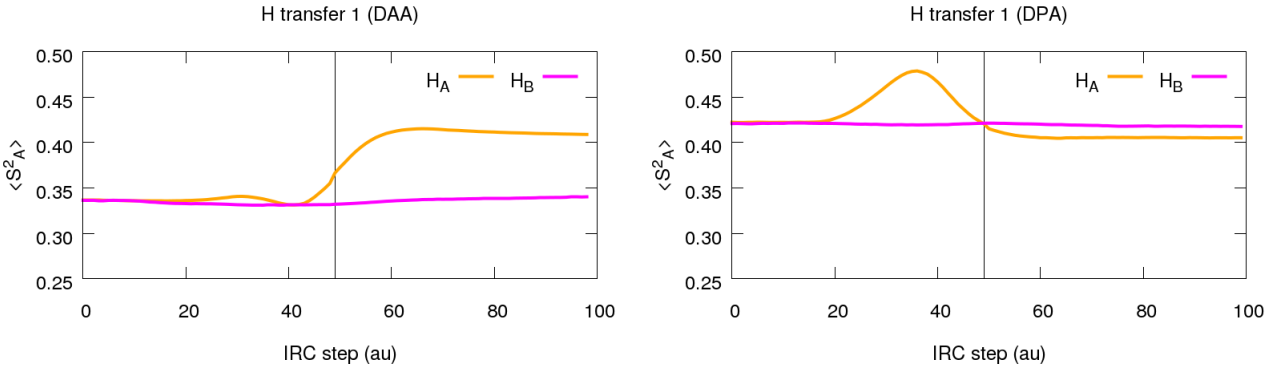

Figure 29: Evolution of the local spin, $< S_A^2 >$, of the H atoms involved in the first H transfer of the DAA and DPA tautomerism.

Second H transfer

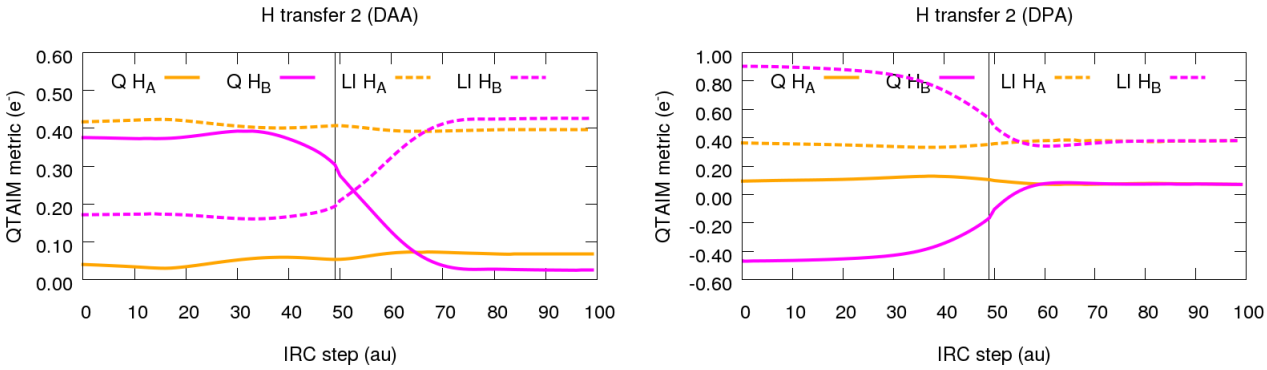

Figure 30: Evolution of the localization index (LI) and atomic charge (Q) of the H_A and H_B atoms throughout the second H transfer involved in the DAA and DPA tautomerism.

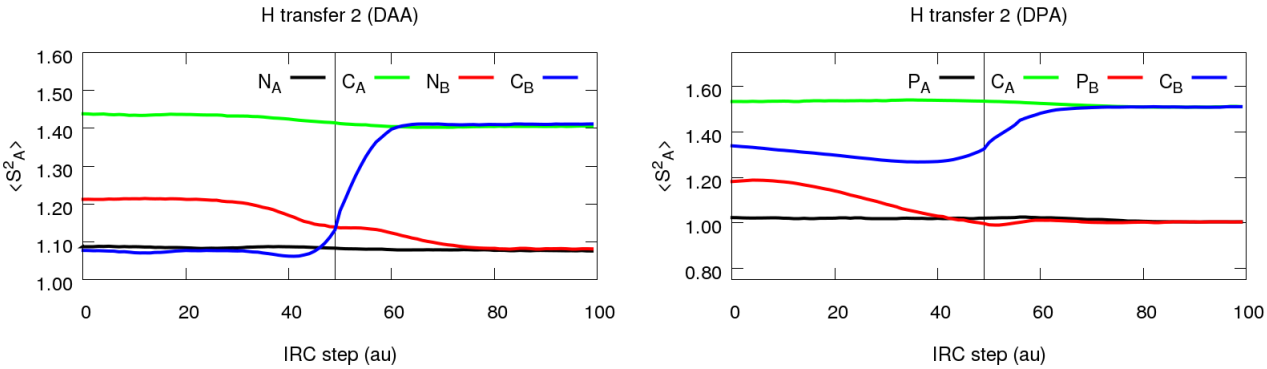

Figure 31: Evolution of the local spin, $< S_A^2 >$, of the main atoms involved in the second H transfer of the DAA and DPA tautomerism.

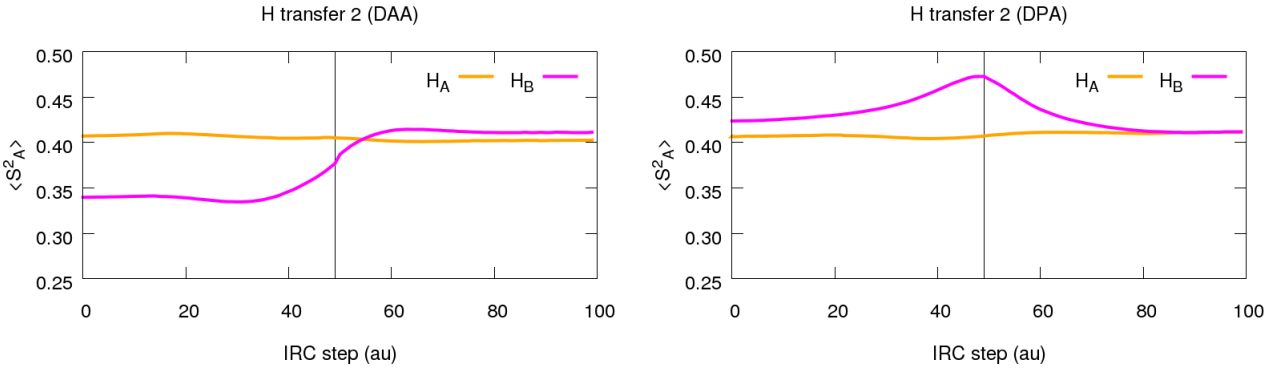

Figure 32: Evolution of the local spin, $< S_A^2 >$, of the H atoms involved in the second H transfer of the DAA and DPA tautomerism.

Local maxima in the $< S_H^2 >$ throughout the DPA tautomerism

As shown in the previous figures, the $< S_H^2 >$ of the H_A and H_B atoms show a very prominent spike in the first and second H transfers, respectively, of the DPA tautomerism. In order to further deepen on the nature of H at these particular geometries, the ELF was computed through single point calculations at such geometries, as shown in the following figures.

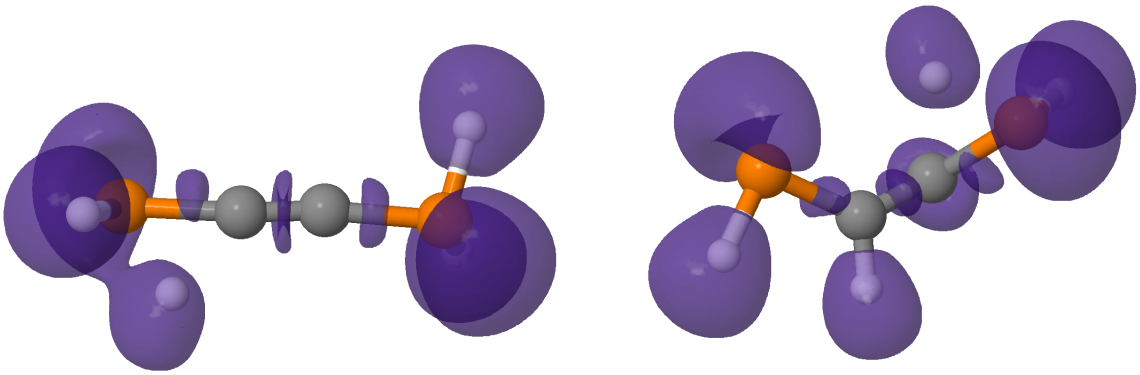

Figure 33: ELF isosurfaces of the intermediate structures, corresponding to the maximum in the $< S_H^2 >$ values, for the first (left) and second (right) H transfer of the DPA tautomerism. An isovalue of 0.86 units was employed throughout.

Similarly, the following table comprises the populations of the V(H) ELF basins at the structures corresponding to the local maxima in $< S_H^2 >$ along with the first and second transition states (TS).

Table 9: Population of the ELF V(H) basins (N) along with its α and β spin contributions for different structures throughout the DPA tautomerism. The labels spk_1 and spk_2 refer to the structures corresponding to the first and second local maxima in the $< S_H^2 >$ values. The restricted (RDFT) and unrestricted (UDFT) solutions are shown. All values are given in electrons.

Structure	N	N_α	N_β
DPA spk_1 (RDFT)	1.64	0.82	0.82
DPA spk_1 (UDFT)	1.64	0.82	0.82
DPA TS_1 (RDFT)	1.76	0.88	0.88
DPA TS_1 (UDFT)	1.76	0.88	0.88
DPA spk_2 (RDFT)	1.63	0.82	0.82
DPA spk_2 (UDFT)	1.63	0.82	0.82
DPA TS_2 (RDFT)	1.61	0.81	0.81
DPA TS_2 (UDFT)	1.61	0.81	0.81

3 Relative stability of DXAs isomers

The following table comprises the relative stability of the here considered isomers of different DXAs.

Table 10: Electronic energies (E) and frequencies (ν_0) of the lowest-lying normal vibration mode of different DXA isomers. The energies are reported relative to those of the linear DXA structure.

Isomer	E (kcal/mol)	ν_0 (cm^{-1})
DAA *butterfly*	30.3	565.14
DAA *cis*	-2.0	106.66
DAA *trans*	-2.3	72.66
DAA *zigzag*	-23.7	174.46
DAA *linear*	0.0	189.45
DPA *butterfly*	-30.1	376.56
DPA *cis*	-9.2	82.84
DPA *trans*	-12.8	72.78
DPA *zigzag*	-10.1	142.6
DPA *linear*	0.0	114.36
DAsA *butterfly*	-41.1	291.99
DAsA *cis*	-18.8	81.13
DAsA *trans*	-21.1	51.27
DAsA *zigzag*	-16.5	123.73
DAsA *linear*	0.0	81.86
DSbA *butterfly*	-48.8	208.94
DSbA *cis*	-20.7	67.78
DSbA *trans*	-21.9	20.8
DSbA *zigzag*	-16.5	109.92
DSbA *linear*	0.0	56.15

4 Cartesian coordinates

The following tables gather the optimized geometries of the DAA isomers, all values are reported in Å.

Table 11: *Butterfly* DAA isomer.

Atom	X	Y	Z
H	2.01050	0.00001	-0.21313
H	-2.01050	-0.00001	-0.21313
H	-1.05605	0.00000	1.36589
H	1.05606	0.00000	1.36589
C	-1.04263	0.00000	0.27517
C	1.04262	0.00000	0.27517
N	-0.00001	0.76275	-0.40054
N	0.00001	-0.76275	-0.40054

Table 12: *Cis* DAA isomer.

Atom	X	Y	Z
H	-2.49288	0.24261	-0.39987
H	2.49289	0.24263	0.39989
H	1.42724	0.96700	-0.96241
H	-1.42720	0.96694	0.96239
C	1.53629	0.29969	-0.10589
C	-1.53629	0.29969	0.10592
N	0.59371	-0.42969	0.32552
N	-0.59371	-0.42966	-0.32555

Table 13: *Trans* DAA isomer.

Atom	X	Y	Z
H	-2.54685	-0.53240	0.00010
H	2.54685	0.53241	-0.00033
H	1.77636	-1.18355	0.00019
H	-1.77636	1.18355	0.00010
C	1.66455	-0.09878	0.00001
C	-1.66455	0.09878	-0.00005
N	0.52962	0.46745	0.00007
N	-0.52962	-0.46745	-0.00004

Table 14: *Zigzag* DAA isomer.

Atom	X	Y	Z
H	2.53398	0.37573	-0.00005
H	0.53331	1.46336	-0.00007
H	-2.53393	-0.37572	-0.00020
H	-0.53336	-1.46336	-0.00006
C	-0.63605	-0.37317	0.00006
C	0.63603	0.37317	0.00003
N	1.73604	-0.25976	-0.00002
N	-1.73603	0.25975	0.00000

Table 15: *Linear* DAA isomer.

Atom	X	Y	Z
C	0.60333	0.00087	-0.00411
C	-0.60333	0.00090	0.00408
N	-1.94875	-0.04708	0.05418
H	-2.42070	-0.43346	-0.74973
H	-2.42083	0.75752	0.43842
N	1.94875	-0.04687	-0.05433
H	2.42069	-0.43622	0.74813
H	2.42082	0.75913	-0.43564

The following tables gather the optimized geometries of the DPA isomers, all values are reported in Å.

Table 16: *Butterfly* DPA isomer.

Atom	X	Y	Z
H	0.00010	2.24062	0.16833
H	-0.00011	-2.24057	0.16826
H	-0.00006	-1.17844	1.64350
H	0.00004	1.17836	1.64348
C	-0.00008	-1.22630	0.55731
C	0.00005	1.22633	0.55730
P	-1.07753	0.00004	-0.34371
P	1.07754	-0.00005	-0.34370

Table 17: *Cis* DPA isomer.

Atom	X	Y	Z
H	2.68312	1.15676	-0.20960
H	-2.68283	1.15749	0.20870
H	-1.03525	1.61610	0.88049
H	1.03536	1.61595	-0.88085
C	-1.63623	0.89735	0.33500
C	1.63614	0.89754	-0.33473
P	-1.08701	-0.54386	-0.29196
P	1.08701	-0.54385	0.29194

Table 18: *Trans* DPA isomer.

Atom	X	Y	Z
H	-3.13768	0.10379	0.00004
H	3.13768	-0.10379	0.00001
H	1.97521	-1.52122	0.00006
H	-1.97521	1.52122	0.00001
C	2.10745	-0.44423	0.00001
C	-2.10745	0.44423	0.00002
P	0.87685	0.68028	-0.00001
P	-0.87685	-0.68028	-0.00001

Table 19: *Zigzag* DPA isomer.

Atom	X	Y	Z
H	2.81419	1.10344	-0.00002
H	0.36968	1.50090	0.00001
H	-2.81421	-1.10341	0.00003
H	-0.36969	-1.50093	0.00000
C	-0.56906	-0.43277	-0.00001
C	0.56905	0.43274	0.00000
P	2.15531	-0.15891	0.00000
P	-2.15530	0.15892	0.00000

Table 20: *Linear* DPA isomer.

Atom	X	Y	Z
C	-0.60650	0.04466	0.02310
C	0.60648	0.04451	-0.02283
P	-2.36057	-0.09143	-0.08754
H	-2.66307	1.29331	-0.15750
H	-2.64010	-0.18986	1.30030
P	2.36060	-0.09094	0.08788
H	2.66310	1.29417	0.14997
H	2.63978	-0.19716	-1.29946

The following tables gather the optimized geometries of the DAsA isomers, all values are reported in Å.

Table 21: *Butterfly* DAsA isomer.

Atom	X	Y	Z
H	0.00001	2.30777	0.38663
H	-0.00000	-2.30775	0.38661
H	0.00001	-1.20981	1.83744
H	-0.00001	1.20979	1.83743
C	0.00000	-1.28669	0.75451
C	0.00000	1.28669	0.75450
As	-1.19407	0.00000	-0.20458
As	1.19407	0.00000	-0.20458

Table 22: *Cis* DAsA isomer.

Atom	X	Y	Z
H	2.67260	1.60013	0.48027
H	-2.67255	1.60018	-0.48031
H	-0.91826	1.97093	-0.89568
H	0.91834	1.97096	0.89568
C	-1.63753	1.27493	-0.48101
C	1.63757	1.27492	0.48101
As	-1.23585	-0.34002	0.16753
As	1.23584	-0.34003	-0.16753

Table 23: *Trans* DAsA isomer.

Atom	X	Y	Z
H	3.15953	-0.94467	-0.00005
H	-3.15953	0.94468	0.00009
H	-1.66004	2.00265	0.00003
H	1.66005	-2.00265	0.00001
C	-2.07675	1.00196	0.00000
C	2.07675	-1.00196	0.00003
As	-1.12050	-0.50827	-0.00001
As	1.12050	0.50827	0.00000

Table 24: *Zigzag* DAsA isomer.

Atom	X	Y	Z
H	2.86350	1.34102	0.00000
H	0.29748	1.51712	0.00000
H	-2.86351	-1.34101	0.00000
H	-0.29748	-1.51713	0.00000
C	-0.53644	-0.45768	0.00000
C	0.53643	0.45767	0.00000
As	2.28260	-0.07652	-0.00000
As	-2.28260	0.07653	-0.00000

Table 25: *Linear* DAsA isomer.

Atom	X	Y	Z
C	-0.60518	0.08185	0.03460
C	0.60518	0.08185	-0.03461
As	-2.49693	-0.05518	-0.04699
H	-2.75234	1.45108	-0.07932
H	-2.70543	-0.12119	1.46545
As	2.49693	-0.05517	0.04700
H	2.75234	1.45110	0.07905
H	2.70542	-0.12146	-1.46543

The following tables gather the optimized geometries of the DSbA isomers, all values are reported in Å.

Table 26: *Butterfly* DSbA isomer.

Atom	X	Y	Z
H	0.00002	2.41214	0.53548
H	-0.00010	-2.41205	0.53535
H	-0.00007	-1.28967	1.95809
H	0.00002	1.28952	1.95804
C	-0.00010	-1.38104	0.87632
C	0.00003	1.38108	0.87629
Sb	-1.37344	0.00001	-0.15199
Sb	1.37345	-0.00001	-0.15198

Table 27: *Cis* DSbA isomer.

Atom	X	Y	Z
H	2.71423	1.98815	-0.63765
H	-2.71427	1.98815	0.63769
H	-0.91637	2.21898	0.92587
H	0.91630	2.21903	-0.92563
C	-1.71379	1.57284	0.57900
C	1.71377	1.57279	-0.57909
Sb	-1.43809	-0.26754	-0.11635
Sb	1.43810	-0.26752	0.11635

Table 28: *Trans* DSbA isomer.

Atom	X	Y	Z
H	-3.14099	0.10072	-0.00060
H	3.14099	-0.10076	0.00073
H	1.96300	-1.52913	0.00125
H	-1.96303	1.52915	-0.00113
C	2.10238	-0.44346	-0.00043
C	-2.10238	0.44345	0.00042
Sb	0.86287	0.68858	-0.00005
Sb	-0.86284	-0.68856	-0.00020

Table 29: *Zigzag* DSbA isomer.

Atom	X	Y	Z
H	3.02909	1.58482	0.00001
H	0.26880	1.52056	0.00000
H	-3.02910	-1.58482	0.00002
H	-0.26880	-1.52057	0.00000
C	-0.51734	-0.46221	-0.00001
C	0.51734	0.46221	-0.00001
Sb	2.49834	-0.05214	0.00000
Sb	-2.49834	0.05215	0.00000

Table 30: *Linear* DSbA isomer.

Atom	X	Y	Z
C	0.60635	0.08620	-0.04004
C	-0.60637	0.08643	0.04032
Sb	2.69753	-0.04010	0.03588
H	2.91975	1.66162	0.00106
H	2.87280	-0.13382	-1.66930
Sb	-2.69751	-0.04033	-0.03571
H	-2.91971	1.66155	-0.01186
H	-2.87338	-0.12318	1.66993

The following tables gather the optimized geometries of the stationary points involved in the DAA tautomerism.

Table 31: Transition state of the first H transfer involved in the DAA tautomerism.

Atom	X	Y	Z
C	0.63064	0.11306	-0.16352
C	-0.59137	0.25033	0.18603
N	-1.83349	-0.13064	-0.01530
H	-2.07536	-0.91733	-0.60297
H	-2.60341	0.38538	0.37713
N	1.95787	-0.16924	-0.03801
H	2.17049	-0.55846	0.88935
H	1.40202	1.00916	-0.42541

Table 32: Reaction intermediate involved in the DAA tautomerism.

Atom	X	Y	Z
C	-0.71469	0.46668	0.16363
C	0.60977	0.50288	-0.42359
N	1.49739	-0.26816	0.12743
H	1.32198	-0.86654	0.93876
H	2.43240	-0.32685	-0.25357
N	-1.62139	-0.41770	-0.02145
H	-1.27483	-1.18100	-0.60917
H	-0.98203	1.35802	0.74194

Table 33: Transition state of the second H transfer involved in the DAA tautomerism.

Atom	X	Y	Z
C	0.65977	0.42928	0.09907
C	-0.57071	-0.31463	0.43490
N	-1.65135	0.17061	-0.22541
H	-1.13858	-0.91295	-0.59747
H	-2.47896	-0.36157	0.07008
N	1.76710	-0.13938	-0.15952
H	1.67235	-1.15443	-0.04919
H	0.60057	1.52244	0.06731

The following tables gather the optimized geometries of the stationary points involved in the DPA tautomerism.

Table 34: Transition state of the first H transfer involved in the DPA tautomerism.

Atom	X	Y	Z
C	-0.64620	-0.20182	0.05841
C	0.59693	0.01529	0.07948
P	2.31049	-0.07502	-0.00605
H	2.71123	0.86836	0.97753
H	2.57567	0.74197	-1.13268
P	-2.38674	0.18621	-0.03021
H	-2.80931	-1.08522	0.44960
H	-1.03837	-1.07385	-0.57784

Table 35: Reaction intermediate involved in the DPA tautomerism.

Atom	X	Y	Z
C	0.70929	0.81060	-0.13749
C	-0.54074	0.62565	0.36115
P	-1.94203	-0.15026	-0.10432
H	-2.60839	-0.57097	1.05673
H	-1.72135	-1.36606	-0.81244
P	2.01493	-0.32076	-0.00008
H	1.22692	-1.42978	0.42915
H	0.99801	1.81468	-0.44935

Table 36: Transition state of the second H transfer involved in the DPA tautomerism.

Atom	X	Y	Z
C	-0.63878	0.70220	-0.08693
C	0.64230	0.65486	0.43286
P	1.95826	-0.25806	-0.21398
H	0.95801	-0.71127	0.86102
H	2.90385	-0.02544	0.83231
P	-1.97146	-0.37584	0.04677
H	-2.87843	0.44173	-0.67980
H	-0.80646	1.66118	-0.58106

The following tables gather the optimized geometries of the stationary points involved in the DAsA tautomerism.

Table 37: Transition state of the first H transfer involved in the DAsA tautomerism.

Atom	X	Y	Z
C	-0.61769	0.37626	-0.05988
C	0.60191	0.06850	-0.19272
As	2.45371	0.02025	0.02367
H	2.78707	-0.91452	-1.13932
H	2.50513	-1.08101	1.07777
As	-2.49477	-0.11883	0.01464
H	-2.94694	1.31989	-0.25275
H	-0.89576	1.26011	0.56563

Table 38: Reaction intermediate involved in the DAsA tautomerism. This structure corresponds to a single point calculation on the pseudo-minimum arising from the IRC calculation.

Atom	X	Y	Z
C	-0.63835	1.06548	-0.15584
C	0.56735	0.96242	0.40164
As	2.01692	-0.13289	-0.06968
H	1.25938	-1.41063	-0.46679
H	2.42811	-0.56568	1.32610
As	-1.99165	-0.25899	0.02678
H	-3.09420	0.70600	-0.42164
H	-1.00127	2.03505	-0.49650

Table 39: Cyclic DAsA structure, resulting from the electrostatically driven ring closure of the intermediate involved in the DAsA tautomerism.

Atom	X	Y	Z
C	-0.73840	1.38560	0.01280
C	0.05529	0.36778	-0.01340
As	1.95325	-0.06421	-0.00933
H	1.81283	-1.30496	-0.88933
H	1.87866	-0.90600	1.26430
As	-1.85571	-0.24957	-0.04807
H	-2.03594	-0.41815	1.47798
H	-0.77582	2.46337	0.04483

Table 40: Transition state of the second H transfer involved in the DAsA tautomerism.

Atom	X	Y	Z
C	-0.60993	0.96777	-0.15510
C	0.63617	1.00142	0.40722
As	2.01321	-0.19469	-0.09979
H	0.86976	-0.33483	1.05944
H	2.98617	0.22388	1.01318
As	-2.01865	-0.23574	0.03605
H	-2.98286	0.60983	-0.79818
H	-0.85105	1.89019	-0.68362

The following tables gather the optimized geometries of the stationary points involved in the DSbA tautomerism.

Table 41: Transition state of the first H transfer involved in the DSbA tautomerism.

Atom	X	Y	Z
C	-0.59542	0.71641	0.00716
C	0.60935	0.40247	0.10377
Sb	2.64393	-0.02255	-0.01852
H	2.43319	-1.38295	-1.04988
H	2.64315	-1.01044	1.38133
Sb	-2.65981	-0.12080	0.00503
H	-3.22901	1.36153	-0.65647
H	-1.12097	1.62923	0.34739

Table 42: Reaction intermediate involved in the DSbA tautomerism. This structure corresponds to a single point calculation on the pseudo-minimum arising from the IRC calculation.

Atom	X	Y	Z
C	-0.61935	1.30751	-0.14250
C	0.54348	1.10521	0.37450
Sb	2.22442	-0.10939	-0.05205
H	1.28328	-1.54848	-0.16908
H	2.61470	-0.39394	1.59030
Sb	-2.20484	-0.20103	0.01007
H	-3.36617	1.03820	-0.27142
H	-1.07509	2.25929	-0.40110

Table 43: Cyclic DAsA structure, resulting from the electrostatically driven ring closure of the intermediate involved in the DSbA tautomerism.

Atom	X	Y	Z
C	-0.69551	1.51622	0.01295
C	0.04412	0.45978	-0.01324
Sb	2.13378	-0.05673	-0.00179
H	1.93354	-1.31943	-1.14565
H	1.94780	-1.16387	1.29505
Sb	-2.07701	-0.17197	-0.03502
H	-2.21624	-0.30361	1.68554
H	-0.65196	2.59489	0.04386

Table 44: Transition state of the second H transfer involved in the DSbA tautomerism.

Atom	X	Y	Z
C	-0.60375	1.16260	-0.16098
C	0.61456	1.16177	0.38485
Sb	2.21720	-0.14972	-0.06618
H	0.78390	-0.28239	1.01340
H	3.14734	0.35801	1.28953
Sb	-2.21377	-0.18400	0.02263
H	-3.26861	0.89429	-0.80205
H	-0.90251	2.10400	-0.62306

5 Additional calculations on reference systems

5.1 ELF topological analyses

The following figures comprise the ELF isosurfaces of the reference systems used to gain insights on the nature of the mechanistic proposals.

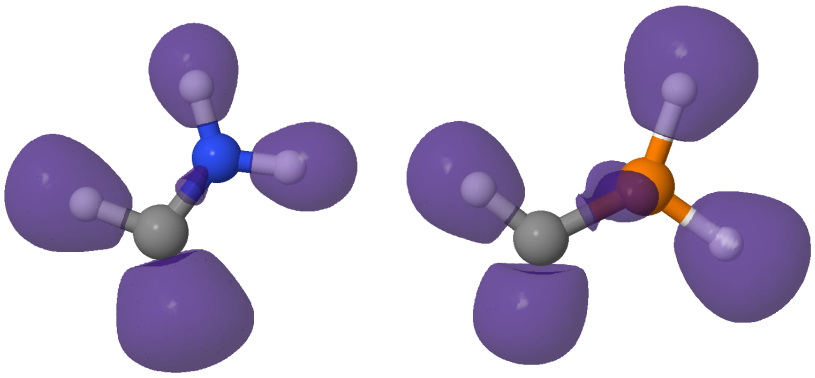

Figure 34: ELF isosurface of the NH_2-CH_2 (left) and PH_2-CH_2 (right) singlet carbenes. An isovalue of 0.86 units was employed.

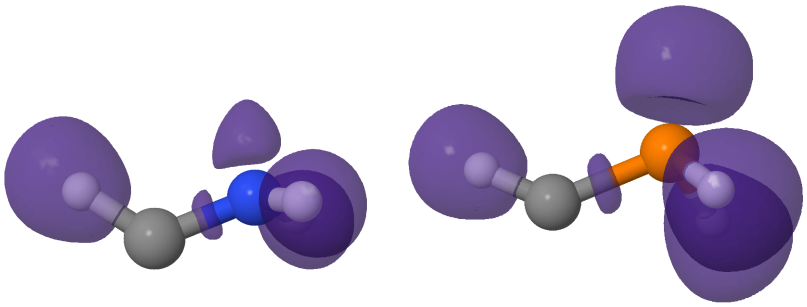

Figure 35: ELF isosurface of the NH_2-CH_2 (left) and PH_2-CH_2 (right) triplet carbenes. An isovalue of 0.86 units was employed.

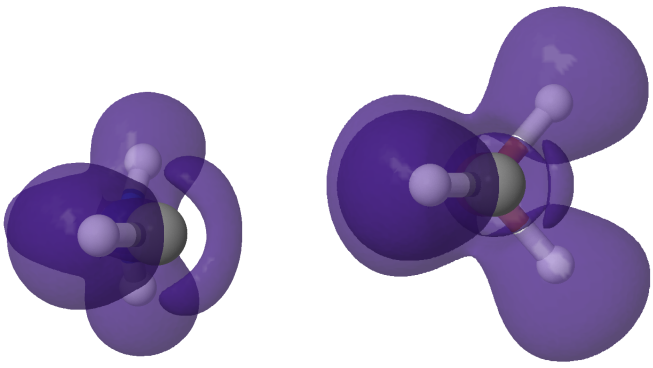

Figure 36: ELF isosurface of the NH_2-CH_2 (left) and PH_2-CH_2 (right) triplet carbenes. An isovalue of 0.76 units was employed.

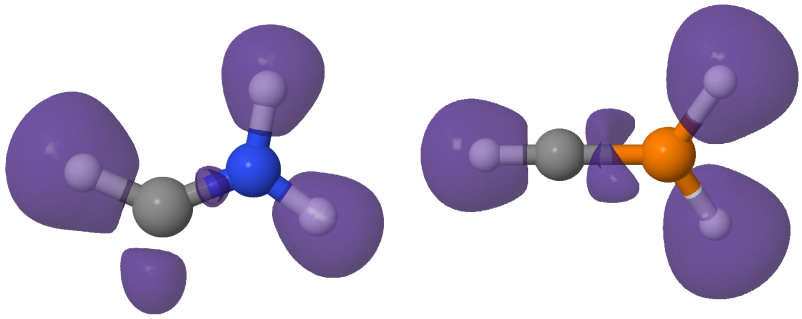

Figure 37: ELF isosurface of the NH_2-CH_2^+ (left) and PH_2-CH_2^+ (right) radical carbocations. An isovalue of 0.86 units was employed.

The following table comprises the total populations (N) along with the α and β spin contributions for the ELF basin of the C atom, V(C), throughout different reference systems.

Table 45: Population of the ELF V(C) basins (N) along with its α and β spin contributions for different reference compounds. All values are reported in electrons.

Compound	N	N_α	N_β
NH_2CH (S=0)	2.22	1.11	1.11
NH_2CH (S=1)	1.93	1.51	0.43
NH_2CH^+ (S=1/2)	1.09	0.82	0.26
PH_2CH (S=0)	2.13	1.07	1.07
PH_2CH (S=1)	1.28	1.02	0.27
PH_2CH^+ (S=1/2)	–	–	–

Similarly, the following table comprises the total populations (N) along with the α and β spin contributions for the ELF basin of the C atom, V(C), throughout the transition states and intermediates involved in the DAA and DPA tautomerism reactions. For each structure, the results for the C atom with a non-bonding ELF valence basins are shown.

Table 46: Population of the ELF V(C) basins (N) along with its α and β spin contributions for the intermediates (inter) and transition states (TS) involved in the DAA and DPA tautomerisms. The restricted (RDFT) and unrestricted (UDFT) solutions are shown. All values are reported in electrons. In the particular case of DPA TS_1, no isolated ELF basins for the C atoms were observed.

Structure	C atom	N	N_α	N_β
DAA TS_1 (RDFT)	C_B	1.65	0.83	0.83
DAA TS_1 (UDFT)	C_B	1.64	0.82	0.82
DAA inter (RDFT)	C_B	2.11	1.05	1.05
DAA inter (UDFT)	C_B	2.11	1.06	1.06
DAA TS_2 (RDFT)	C_B	2.06	1.03	1.03
DAA TS_2 (UDFT)	C_B	2.06	1.03	1.03
DPA TS_1 (RDFT)	–	–	–	–
DPA TS_1 (UDFT)	–	–	–	–
DPA inter (RDFT)	C_B	1.77	0.88	0.88
DPA inter (UDFT)	C_B	1.77	0.88	0.88
DPA TS_2 (RDFT)	C_B	1.86	0.93	0.93
DPA TS_2 (UDFT)	C_B	1.86	0.93	0.93

5.2 Local spin $< S_A^2 >$ calculations

The following tables comprise the value of the local spin, $< S_A^2 >$, of some the most relevant atoms of the test-bed reference systems.

Table 47: Local spin of the C and H atoms, computed at the B3LYP/def2-TZVP level of theory, of different hydrocarbons.

Compound	$< S_C^2 >$	$< S_H^2 >$
CH_4	1.48	0.41
CH_3-CH_3	1.52	0.42
CH_2=CH_2	1.49	0.41
CH≡CH	1.46	0.39

Table 48: Local spin of the C, H and X atoms, computed at the B3LYP/def2-TZVP level of theory, of different amino- and phosphino- derivatives. The label α is used to refer to the C atom directly bonded to the XH_2 group (X= N or P).

Compound	$< S_C^2 >$ (C_α)	$< S_H^2 >$ (C_α-H)	$< S_X^2 >$	$< S_H^2 >$ (X-H)
NH_2CH_2-CH_3	1.51	0.42	1.14	0.35
NH_2CH=CH_2	1.48	0.41	1.15	0.34
NH_2C≡CH	1.47	–	1.14	0.33
PH_2CH_2-CH_3	1.56	0.42	1.05	0.42
PH_2CH=CH_2	1.53	0.41	1.03	0.42
PH_2C≡CH	1.48	–	0.99	0.42

Table 49: Local spin of the C and H atoms, computed at the B3LYP/def2-TZVP level of theory, of the singlet (S=0) and triplet (S=1) CH_2 carbenes along with the CH_2^+ radical.

Compound	$< S_C^2 >$	$< S_H^2 >$
CH_2 (S=0)	0.78	0.41
CH_2 (S=1)	2.47	0.41
CH_2^+ (S=1/2)	1.29	0.33

Table 50: Local spin of the C, H and X atoms, computed at the B3LYP/def2-TZVP level of theory, of the singlet (S=0) and triplet (S=1) XH_2-CH carbenes along with the XH_2-CH^+ radical. The label α is used to refer to the C atom directly bonded to the XH_2 group (X= N or P).

Compound	$< S_C^2 >$ (C_α)	$< S_H^2 >$ (C_α-H)	$< S_X^2 >$	$< S_H^2 >$ (X-H)
NH_2CH (S=0)	0.94	0.41	1.20	0.33
NH_2CH (S=1)	2.07	0.42	1.22	0.34
NH_2CH^+ (S=1/2)	1.44	0.35	1.17	0.28
PH_2CH (S=0)	2.22	0.41	1.09	0.42
PH_2CH (S=1)	1.20	0.41	1.33	0.42
PH_2CH^+ (S=1/2)	1.61	0.35	1.23	0.41

References

[1] M. J. Frisch, G. W. Trucks, H. B. Schlegel, G. E. Scuseria, M. A. Robb, J. R. Cheeseman, G. Scalmani, V. Barone, B. Mennucci, G. A. Petersson, H. Nakatsuji, M. Caricato, X. Li, H. P. Hratchian, A. F. Izmaylov, J. Bloino, G. Zheng, J. L. Sonnenberg, M. Hada, M. Ehara, K. Toyota, R. Fukuda, J. Hasegawa, M. Ishida, T. Nakajima, Y. Honda, O. Kitao, H. Nakai, T. Vreven, J. A. Montgomery, Jr., J. E. Peralta, F. Ogliaro, M. Bearpark, J. J. Heyd, E. Brothers, K. N. Kudin, V. N. Staroverov, R. Kobayashi, J. Normand, K. Raghavachari, A. Rendell, J. C. Burant, S. S. Iyengar, J. Tomasi, M. Cossi, N. Rega, J. M. Millam, M. Klene, J. E. Knox, J. B. Cross, V. Bakken, C. Adamo, J. Jaramillo, R. Gomperts, R. E. Stratmann, O. Yazyev, A. J. Austin, R. Cammi, C. Pomelli, J. W. Ochterski, R. L. Martin, K. Morokuma, V. G. Zakrzewski, G. A. Voth, P. Salvador, J. J. Dannenberg, S. Dapprich, A. D. Daniels, O. Farkas, J. B. Foresman, J. V. Ortiz, J. Cioslowski and D. J. Fox, *Gaussian 09 Revision E.01*, Gaussian Inc. Wallingford CT 2009.